

# A short distance quark-antiquark potential

A.M. Badalian and D.S. Kuzmenko

*Institute of Theoretical and Experimental Physics,  
117218, B.Cheremushkinskaya 25, Moscow, Russia*

## Abstract

Leading terms of the static quark-antiquark potential in the background perturbation theory are reviewed, including perturbative, nonperturbative and interference ones. The potential is shown to describe lattice data at short quark-antiquark separations with a good accuracy.

1. The static quark-antiquark potential was calculated with high accuracy in lattice QCD some years ago [1]. It was shown to be well described by the phenomenological Coulomb+linear Cornell potential at sufficiently large quark-antiquark separations,  $R \gtrsim 0.2$  fm. At smaller distances the Cornell potential is not applicable. The region  $0.03 \text{ fm} \leq R \leq 0.22 \text{ fm}$  was studied in quenched lattice theory in detail [2], and the conclusion was made that the standard perturbative theory expansion in coupling constant does not yield appropriate description of lattice results, at least in one- and two-loop approximations. As is known, next terms of the asymptotic coupling expansion depend on the renormalization scheme, and so the corresponding static potential does. One can argue that the standard perturbative theory fails because this region is close to the unphysical Landau pole of the strong coupling.

We consider the static quark-antiquark potential in the background perturbation theory (BPT) [3]. This potential incorporates both the features of the standard perturbative potential at tiny distances,  $R \lesssim 0.05$  fm, and of the Cornell potential at  $R \gtrsim 0.4$  fm due to taking nonperturbative background field effects into account. After brief review of leading background potential terms we present our results concerning the behavior of the potential at short distances and its comparison with the lattice [4].

2. The gluon field  $A_\mu$  in BPT is divided into the dynamical perturbative part  $a_\mu$  and the background nonperturbative field  $B_\mu$ ,

$$A_\mu = a_\mu + B_\mu. \quad (1)$$

The background field, in which perturbative valence gluons propagate, results in the vacuum condensate creation.

The static potential has to be calculated using the vacuum averaged Wilson loop for the quark-antiquark pair. The BPT Wilson loop expansion in the field  $a_\mu$  has the form [3]

$$W(B + a) = W(B) + \sum_{n=1}^{\infty} (ig)^n W^{(n)}(B; x(1)...x(n)) a_{\mu_1} ... a_{\mu_n} dx_{\mu_1}(1) ... dx_{\mu_n}(n). \quad (2)$$

To perform the averaging of the expression (2), we take into account that the linear in  $a_\mu$  term vanishes,

$$\langle W(B + a) \rangle_{B,a} = \langle W(B) \rangle_B - g^2 \left\langle W^{(2)}(B; x, y) \right\rangle_B dx dy + ..., \quad (3)$$

where

$$-g^2 W^{(2)} dx dy = -g^2 \int \Phi^{\alpha\beta}(x, y, B) t_{\delta\alpha}^a t_{\beta\gamma}^b G_{\mu\nu}^{ab}(x, y, B) \Phi^{\gamma\delta}(y, x) dx_\mu dy_\nu. \quad (4)$$

The Green function of the valence gluon in the background gauge takes the form [3]

$$G_{\mu\nu}(x, y) = \langle a_\mu(x) a_\nu(y) \rangle_B = \langle x | (\hat{D}_\lambda^2 \cdot \delta_{\mu\nu} - 2ig \hat{F}_{\mu\nu})^{-1} | y \rangle, \quad (5)$$

where  $\hat{D}_\lambda^2$  is the covariant derivative depending on the field  $B$ , and  $\hat{F}_{\mu\nu}$  is the background field strength. The operator  $\hat{F}_{\mu\nu}$  has to be considered as a correction [3]. The Green function expansion in the  $\hat{F}_{\mu\nu}$  takes the form

$$G(x, y) = \langle x | D^{-2} | y \rangle - \langle x | D^{-2} 2ig \hat{F} D^{-2} | y \rangle + \langle x | D^{-2} 2ig \hat{F} D^{-2} 2ig \hat{F} D^{-2} | y \rangle + \dots \quad (6)$$

The terms of odd powers in the field  $B$  vanish. Let us confine ourselves by the third term in the expansion (6) and quadratic term in (3), and write the Wilson loop in the form

$$\langle W(B + a) \rangle_{B,a} \simeq \langle W(B) \rangle_B + \langle W(B) \rangle_B (\tilde{W}_1^{(2)} + \tilde{W}_3^{(2)}). \quad (7)$$

One can verify using the Fock-Feynman-Schwinger representation [6] for the Green function expansion (6) that the factorization of the second term in (7) is valid. Terms proportional to  $\tilde{W}_1^{(2)}$  and  $\tilde{W}_3^{(2)}$  come from the first and third terms in (6). The following approximate expression is valid within the accuracy considered,

$$\langle W(B + a) \rangle_{B,a} \simeq \langle W(B) \rangle_B \exp(\tilde{W}_1^{(2)} + \tilde{W}_3^{(2)}). \quad (8)$$

Taking the logarithm, we arrive at the three corresponding terms in the static potential,

$$V_{Q\bar{Q}}(r) = -\lim_{T \rightarrow \infty} \frac{1}{T} \ln \langle W(B + a) \rangle_{B,a} = V_{NP}(r) + V_P(r) + V_{\text{int}}(r), \quad (9)$$

where  $r$  is the quark-antiquark separation, the nonperturbative potential  $V_{NP}$  is given by the average of the Wilson loop  $\langle W(B) \rangle_B$ , the background perturbative potential  $V_P$  comes from the first term in the expansion (6), and the interference potential  $V_{\text{int}}$  comes from the third one. The nonperturbative potential rises linearly at distances  $r \gtrsim T_g$ , where  $T_g = 0.12 \div 0.2$  fm is the background field correlation length, and is quadratic at short distances  $r \lesssim T_g$  (see e.g. the talk at this conference [7]),

$$V_{NP}(r) \simeq \frac{2}{\pi} \frac{r}{T_g} \sigma r. \quad (10)$$

One can see that at short distances  $V_{NP}(r) \ll \sigma r$ .

The interference potential was calculated in [8] and shown to be close to the linear one at short distances,

$$V_{\text{int}}(r) \simeq \sigma R. \quad (11)$$

The background perturbative potential has the form [3]

$$V_P(r) = -\frac{C_F \alpha_B(r)}{r}, \quad (12)$$

where  $C_F = 4/3$  and the background coupling  $\alpha_B(r)$  saturates with some critical, or freezing, value at large  $r$ .

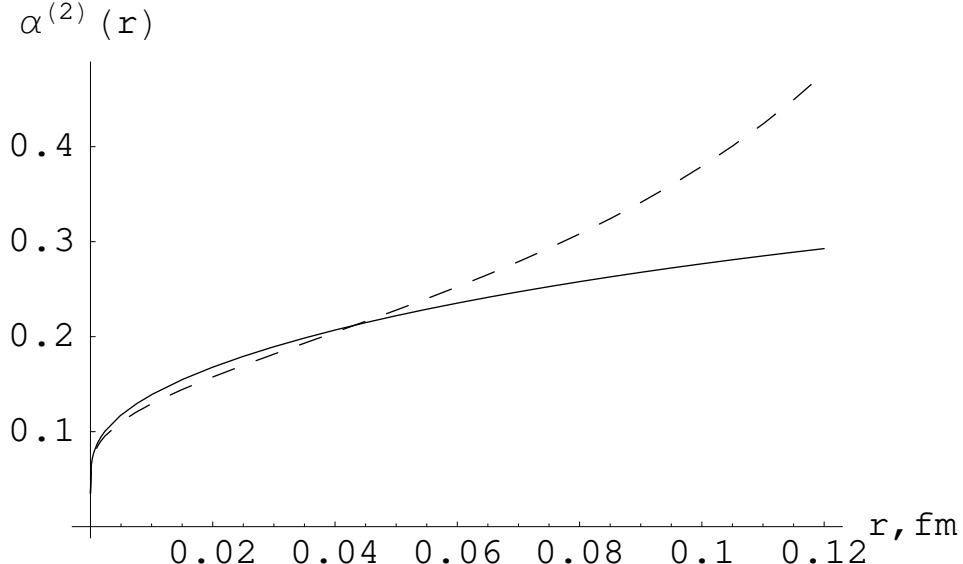


Figure 1: The background coupling  $\alpha_B^{(2)}(r)$  with  $\Lambda = 385$  MeV,  $m_B = 1.0$  GeV (solid line) compared to the perturbative  $\alpha_s^{(2)}(r)$  with  $\Lambda_R = 686$  MeV (dashed line) at short distances. A rigorous definition of  $\alpha_s(r)$  and  $\Lambda_R$  is given in [4].

3. We proceed now to a comparison between background and standard couplings at short distances. The Callan-Symanzik equation yields the following expressions for the running coupling constant in one- and two-loop approximations,

$$\alpha_s^{(1)}(q) = \frac{4\pi}{\beta_0 \ln \frac{q^2}{\Lambda^2}}, \quad (13)$$

$$\alpha_s^{(2)}(q) = \alpha_s^{(1)}(q) \left( 1 - \frac{\beta_1}{\beta_0^2} \frac{\ln \ln \frac{q^2}{\Lambda^2}}{\ln \frac{q^2}{\Lambda^2}} \right), \quad (14)$$

where  $\beta_0 = 11 - \frac{2}{3}n_f$ ,  $\beta_1 = 102 - \frac{38}{3}n_f$ ,  $q^2 \equiv \mathbf{q}^2$  and  $\Lambda \approx 385$  MeV is the QCD constant (for the discussion of its value see [4]).

The modified Callan-Symanzik equation is used in BPT [3] for the background coupling  $\alpha_B$ , which takes into account the background field contribution and leads to the substitution  $q^2 \rightarrow q^2 + m_B^2$  in (13), (14), where  $m_B = 1$  GeV [4]. One can see that the background coupling saturates with the freezing value in infrared region  $q^2 \ll m_B^2$  and turns to standard  $\alpha_s$  in ultraviolet one.

The background coupling in the coordinate representation can be calculated using the Fourier transform, and in two-loop approximation takes the form

$$\alpha_B^{(2)}(r) = \frac{8}{\beta_0} \int_0^\infty \frac{dq}{q} \frac{\sin qr}{\ln \frac{q^2 + m_B^2}{\Lambda^2}} \left( 1 - \frac{\beta_1}{\beta_0^2} \frac{\ln \ln \frac{q^2 + m_B^2}{\Lambda^2}}{\ln \frac{q^2 + m_B^2}{\Lambda^2}} \right). \quad (15)$$

It is shown in comparison with the standard coupling in Fig. 1. One can see from the figure considerable difference between two curves at  $r \gtrsim 0.05$  fm. The coupling  $\alpha_s(r)$  grows rapidly in this region due to the influence of the pole, which is situated at  $r \simeq 0.3$  fm.

Let us compare now the background static potential behavior at short distances with the lattice one.

Relying on the relations (9)-(12), (15), we approximate the potential in this region by the sum [4]

$$V_B(r) \approx -\frac{4}{3} \frac{\alpha_B^{(2)}(r)}{r} + \sigma r. \quad (16)$$

The behavior of  $V_B(r)$  at  $r < 0.22$  fm is shown in Fig. 2 in comparison with lattice points from [2]. The values of  $\sigma = 0.2$  GeV<sup>2</sup> and overall shift  $C = -253$  MeV were taken from the fit, which has provided agreement between background and lattice potentials with the accuracy  $\lesssim 50$  MeV of the latter.

4. In summary we enumerate some properties of the short distance static quark-antiquark potential.

- The potential at  $r \ll T_g$  consists mainly of perturbative and interference parts. Purely nonperturbative potential is small in this region.
- The background running coupling constant saturates with the freezing value in infrared region and goes over to the standard coupling in ultraviolet region.
- A considerable difference between standard and background couplings in two-loop approximation starts already at distances  $r \gtrsim 0.05$  fm.
- The background potential, approximated as a sum of two-loop background perturbative potential and linear potential with the slope  $\sigma$ , yields a good description of lattice simulations at short distances. This in turn means that the short distance area law for the Wilson loop, used in particular in the QCD string approach [5], is justified.

This work has been supported by RFBR grants 00-02-17836, 00-15-96786, and INTAS 00-00110, 00-00366.

## References

- [1] G.S.Bali, Phys.Rept. **343**, 1 (2001).
- [2] G.S.Bali, Phys. Lett. **B460**, 170 (1999).
- [3] Yu.A.Simonov, in: Lecture Notes in Physics, v.479 p.139 (1996), Springer-Verlag, Berlin-Heidelberg; Phys.At.Nucl. **58**, 107 (1995).
- [4] A.M.Badalian and D.S.Kuzmenko, Phys.Rev. **D65**, 016004 (2002).
- [5] Yu.S. Kalashnikova and D.S. Kuzmenko, this volume, hep-ph/0302070.
- [6] Yu.A.Simonov and J.A. Tjon, Annals Phys. **300**, 54 (2002).
- [7] D.S. Kuzmenko, this volume, hep-ph/0302067.
- [8] Yu.A.Simonov, Phys.Rept. 320, 265 (1999)

## Figure caption

Figure 2: The background potential  $V_B(r)$  (solid line) compared to the lattice one from [2] (points) in units of  $r_0 = 2.5 \text{ GeV}^{-1}$ . 1-loop and 2-loop standard perturbative potentials from [2] are shown by thin solid line below lattice points and dash-dotted line correspondingly; 1-loop + linear with the large slope  $\sigma^* \approx 1 \text{ GeV}^2$  potential is shown by dashed line. The figure is taken from our paper [4].

This figure "Figure2.gif" is available in "gif" format from:

<http://arxiv.org/ps/hep-ph/0302072v1>